MSDE

PAPER

Optimization of chondroitin production in *E. coli* using genome scale models†

Márcia R. Couto, [ID][a] Joana L. Rodrigues, [ID]*[ab] Adelaide Braga, [ID][ab] Oscar Dias [ID][ab] and Lígia R. Rodrigues [ID][ab]

Chondroitin is a natural occurring glycosaminoglycan with applications as a nutraceutical and pharmaceutical ingredient and can be extracted from animal tissues. Microbial chondroitin-like polysaccharides emerged as a safer and more sustainable alternative source. However, chondroitin titers using either natural or recombinant microorganisms are still far from meeting the increasing demand. The use of genome-scale models and computational predictions can assist the design of microbial cell factories with possible improved titers of these value-added compounds. Genome-scale models have been herein used for the first time to predict genetic modifications in *Escherichia coli* engineered strains that would potentially lead to improved chondroitin production. Additionally, using synthetic biology approaches, a pathway for producing chondroitin has been designed and engineered in *E. coli*. Afterwards, the most promising mutants identified based on bioinformatics predictions were constructed and evaluated for chondroitin production in flask fermentation. This resulted in the production of 118 mg L^{-1} of extracellular chondroitin by overexpressing both superoxide dismutase (*sodA*) and a lytic murein transglycosylase (*mltB*). Then, batch and fed-batch fermentations at the bioreactor scale were also evaluated, in which the mutant overexpressing *mltB* led to an extracellular chondroitin production of 427 mg L^{-1} and 535 mg L^{-1}, respectively. The computational approach herein described identified several potential novel targets for improved chondroitin biosynthesis, which may ultimately lead to a more efficient production of this glycosaminoglycan.

Design, System, Application

Chondroitin sulfate, a polysaccharide with several medical, veterinary, pharmaceutical, and cosmetic applications, is traditionally extracted with low yields from animal sources raising religious and ethical concerns. Efforts to produce chondroitin in an economic and safer way have been conducted by constructing artificial biosynthetic pathways in heterologous microbial hosts but the yields still do not meet the growing demand. *Escherichia coli* is the most studied host for chondroitin production as there are many pathogenic strains that naturally produce it. In this study, synthetic biology approaches were used to design and construct a biosynthetic pathway for chondroitin production in *E. coli*. Genome-scale models were used to predict genetic modifications (gene deletion, gene under or overexpression) in *E. coli* engineered strains that could potentially lead to an improved chondroitin production. The most promising mutants identified based on *in silico* predictions were constructed and further evaluated for chondroitin production exhibiting improved productions compared to the control strain harboring only the chondroitin pathway. The findings of this study shed light on novel metabolic engineering targets to improve chondroitin production, contributing to advancements in the biotechnological production of this highly sought glycosaminoglycan.

Introduction

Genome-scale metabolic models (GEMs) are mathematical representations of the entire metabolic network of an organism (or consortium), which include a description of genes, enzymes, reactions, and metabolites, as well as their associations and compartments, ultimately allowing the prediction of biological capabilities.[1] Along with the increasing knowledge and data provided by genome sequencing technologies, the number, quality, and applications of available GEMs have been growing. These models provide valuable information for metabolic engineering strategies as they allow the prediction of phenotypic behavior of either wild-type or mutated strains under different environmental conditions and identification of targets to improve the metabolic flux towards a target product.[2,3] Applications of GEMs on drug target identification/drug discovery/drug design and human disease

[a] *Centre of Biological Engineering, University of Minho, Braga, Portugal.*
E-mail: joanarodrigues@deb.uminho.pt

[b] *LABBELS – Associate Laboratory, BragaGuimarães, Portugal*

This journal is © The Royal Society of Chemistry and IChemE 2024

Mol. Syst. Des. Eng., 2024, 9, 597–611 | 597

studying have also been described.[2] The BiGG Models repository[4] currently provides 108 open-source manually curated GEMs that exhibit robustness of growth predictions.

The phenotype can be estimated by different tools. Flux balance analysis (FBA) is a common mathematical method for analyzing the flux distributions through the metabolic network. This approach relies on mass balance equations assuming steady-state growth (all mass that enters the system must leave, so no metabolite is accumulated).[1] Considering the constraints imposed by mass balance equations, environmental conditions and model metabolic bounds, FBA computes a possible flux distribution by maximizing an objective function by linear programming. Commonly, the biomass production reaction/equation is used as the objective function for simulating microbial phenotypes. FBA accurately predicts wild-type behavior, although for mutant phenotype prediction the simulation methods minimization of metabolic adjustment (MOMA)[5] and linear MOMA (LMOMA)[6,7] have been more frequently used. These methods assume that engineered strains will no longer grow to optimize biomass, but instead they grow to maintain the flux distribution as close to the wild-type as possible.

While simulation methods are essential for phenotype prediction, finding combinations of genetic modifications to reach a desired phenotype requires more complex computational tools to iteratively generate and evaluate candidate solutions until a desired phenotype or other termination criteria are achieved.[8] Examples of such computational strain optimization methods include OptKnock,[9] OptStrain,[10] OptGene,[11] simulated annealing/evolutionary algorithms (SA/SEA),[12] FluxDesign,[13] OptORF[14] and OptForce.[15] These tools differ in the defined objective function, optimization algorithms, simulation methods, the information they support, and/or in the mathematical formulation.[8]

Biological behavior prediction through computational modulation has been widely and successfully used to increase the biotechnological production of several high-value compounds such as fatty acids,[16] organic acids,[17-20] lipids,[21-23] polymers,[3,24-26] amino acids,[27] butanol,[28] naringenin[29] and glycosaminoglycan hyaluronic acid.[30]

As reviewed in ref. 31, chondroitin and chondroitin-derived compounds are glycosaminoglycans (GAG) with several applications. Chondroitin sulfate is mainly used as a chondroprotective ingredient in human and veterinary medical prescriptions.[31] The usual chondroitin sulfate source in current chondroitin-based market products is cartilages such as shark or cows, and efforts are being implemented to shift the production process to a more sustainable and safer one such as biological production using microorganisms.[31] Several pathogenic bacteria (e.g., Pasteurella multocida) are natural producers of chondroitin, also called unsulfated chondroitin, and the pathways are currently well-defined. This opened the possibility of using genetic engineering to produce these compounds in a safer and more sustainable way. Biotechnological chondroitin is frequently converted to chondroitin sulfate by an additional step performed by mammalian sulfotransferases. However, in the last few years several studies concluded that this compound, as chondroitin sulfate, also has very interesting biological properties, such as anti-inflammatory, that can be applied in osteoarthritis treatment.[32-35] Despite the advances in the biotechnological production of chondroitin and chondroitin sulfate it remains challenging, mainly due to the low titers obtained.[36] Strategies to improve microbial strains for producing chondroitin and its derivatives are therefore essential. Escherichia coli has been the most widely used and well-known host for biotechnological applications, participating as a living catalyst in well-established industrial processes. Therefore, this microorganism was herein used as the host for heterologous chondroitin production in silico and in vivo. As far as we know, this was the first time GEMs have been used to predict chondroitin production. The identified targets can guide future works towards more efficient hosts for chondroitin production.

Experimental

Model construction and computational approach

E. coli BL21's stoichiometric models iEC1356_Bl21DE3, iB21_1397, iECBD_1354 and the parent model iJO1366, from E. coli K-12, were obtained from the BiGG Models database (https://bigg.ucsd.edu/). These models were modified to include the heterologous pathway for chondroitin production in silico. The included reactions were uridine-diphosphate (UDP)-N-acetylglucosamine 4-epimerase (UAE), chondroitin synthase/polymerase (CHSY) and their corresponding genes, as well as a chondroitin exchange reaction. Chondroitin was added as new species in all models, and UDP-N-acetyl-D-galactosamine was also included, except for the iEC1356_Bl21DE3 model that already contained this intermediate. The resulting models harboring the chondroitin pathway were named iEC1356_Bl21DE3_c, iB21_1397_c, iECBD_1354_c and iJO1366_c.

The modified models were uploaded/imported in the workbench OptFlux Version 3.3.5.[37] The Linear Programming solver employed in this study was CPLEX Optimization Studio Version 12.9.0, developed by IBM. Evolutionary optimization was performed for gene deletion and for gene under and overexpression predictions, to search for mutants with enhanced flux for the chondroitin production reaction. The optimization method employed in this study was the strength Pareto evolutionary algorithm 2 (SPEA2). Optimizations were performed with parsimonious FBA (pFBA)[38] and using the biomass-product coupled yield (BPCY) as the objective function. The maximum for evaluation functions was set to 50 000. A maximum of 10 modifications was allowed. The environmental conditions were set to aerobic (without any restriction of oxygen, lower bound set to −1000) and the substrate glucose to 10 mmol gDW^{-1} h^{-1} (lower bound set to −10).

598 | Mol. Syst. Des. Eng., 2024, 9, 597–611

This journal is © The Royal Society of Chemistry and IChemE 2024

A recently described alternative computational approach was also performed using the MEWpy workbench developed for Python[39] (the XML file is available in ESI† S2). *E. coli* BL21 model iB21_1397 was used for this approach. Under identical environmental conditions as previously described, the evolutionary optimization was conducted using a multi-objective approach. The objectives were set as the BPCY and the weighted yield (WYIELD), representing the weighed sum of the minimum and maximum product fluxes. pFBA was used as the phenotype prediction method and the evolutionary algorithm (EA) Non-dominated sorting genetic algorithm II[40] was used for the optimization approach.

To evaluate the robustness of the obtained solutions from strain optimization, flux variability analysis (FVA) was performed by fixing biomass as the obtained in the mutant solution and alternating the pFBA objective function between maximizing and minimizing chondroitin production.[41]

Heterologous pathway construction

The strains and plasmids used to construct a chondroitin production pathway *in vivo* in *E. coli* are described in Table 1. The pathway contained three genes for the expression of UDP-glucose dehydrogenase (UGD), UAE and CHSY. The selected genes to perform UAE and CHSY enzymatic reactions were the ones from the pathogenic strain *E. coli* O5:K4:H4 which naturally produces a compound analogue to chondroitin as part of its capsule.[42] The genes *kfoA* and *kfoC* (encoding UAE and CHSY, respectively) present in the pETM6 plasmid were kindly provided by Dr. Matheos Koffas (Rensselaer Polytechnic Institute, Troy, NY)[36] and were cloned in pRSFDuet-1 plasmid (Novagen, Madison, USA) in multiple cloning site 1 (MCS1). Also, since the UGD overexpression has been determined to be crucial for glycosaminoglycan production,[43–46] *Zymomonas mobilis* UGD gene (*Zmugd*)[46] was also cloned in the same plasmid in MCS2. The three genes were cloned in pseudo-operon configuration, *i.e.*, the DNA sequence of each gene follows its own lac operator, T7 promoter and RBS, and a single T7 terminator exists in the end of all genes.

Plasmid DNA was extracted using the NucleoSpin® Plasmid Miniprep Kit (Macherey-Nagel, Düren, Germany). Genes have been amplified using Phusion High Fidelity DNA Polymerase (Thermo Fisher Scientific, Waltham, USA) and the primers (Metabion, Steinkirchen, Germany; Eurofins, Ebersberg, Germany) are described in Table S1.† Amplified DNA fragments were purified from agarose using NucleoSpin® Gel and PCR Clean-up Kit (Macherey-Nagel). Plasmid DNA and PCR products were quantified using a NanoDrop One instrument (Thermo Fisher Scientific) and were digested with the suitable restriction endonucleases (Thermo Fisher Scientific) for 1 h at 37 °C and purified using NucleoSpin® Gel and PCR Clean-up Kit. Ligations were performed for 1 h at room temperature using a T4 DNA ligase (Thermo Fisher Scientific). The constructions were transformed by heat shock into *E. coli* NZY5α competent cells (NZYTech, Lisbon, Portugal). Super optimal broth with catabolite repression (SOC; NZYTech) was used for transformant recovery.

All plasmids herein constructed were verified by colony PCR using Dream *Taq* polymerase (Thermo Fisher Scientific) and digestion, and their sequences were further confirmed by sequencing (Eurofins) (Primers in Table S1†). After sequence confirmation, the resulting plasmid with the assembled pathway, pRSFDuet_kfoCA_Zmugd, was transformed in *E. coli* K-12 MG1655 (DE3) and *E. coli* BL21 (DE3) strains for the evaluation of chondroitin production.

Mutant construction

The evaluated modifications to improve heterologous chondroitin production included membrane-bound lytic murein transglycosylase B (*mltB*), superoxide dismutase (*sodA*) and *N*-acetylglucosamine-1-phosphate uridyltransferase (*glmU*) overexpression, sugar phosphatase (*ybiV*) and lipid II flippase (*murJ*) underexpression, and β-*N*-

Table 1 Strains and plasmids used in this study

Strains	Relevant genotype	Source
Escherichia coli NZY5α	*fhuA2* Δ(*argF-lacZ*)U169 *phoA glnV44*Φ80 Δ(*lacZ*)M15 *gyrA96 recA1 relA1 endA1 thi-1 hsdR17*	NZYTech (MB00401)
E. coli K-12 MG1655 (DE3)	F- λ- *ilvG- rfb*-50 *rph*-1 λ(DE3)	49
E. coli BL21 (DE3)	F- *ompT gal dcm lon hsdSB*(rB- mB-) λ(DE3 *lacI lacUV5-T7* gene 1 *ind1 sam7 nin5*)	NZYTech (MB006)

Plasmids	Description	Source
pRSFDuet-1	RSF1030 *ori*, *lacI*, double P$_{T7lac}$, Kan^R	Novagen
pRSFDuet_Zmugd	pRSFDuet-1 carrying *Z. mobilis* UGD (*ZmUGD*) gene in the MCS1	46
pETM6_PCA	pETM6 harboring the genes *kfoC*, *kfoA* from *E. coli* K4 in pseudo-operon configuration	36
pRSFDuet_kfoCA_Zmugd	pRSFDuet-1 harboring *kfoA* and *kfoC* in MCS1 and *Zmugd* in MCS2	This study
pETDuet-1	ColE1(pBR322) *ori*, *lacI*, double P$_{T7lac}$, Amp^R	Novagen
pCDFDuet-1	CloDF13 *ori*, *lacI*, double P$_{T7lac}$, Strep^R	Novagen
pCRISPathBrick	P15A ori, Cm^R, expression of *S. pyogenes* dCas9, tracrRNA, and nontargeting CRISPR array	Addgene #65006
pETDuet_sodA	pETDuet-1 harboring *sodA* from *E. coli* K-12 MG1655 (DE3)	This study
pETDuet_glmU	pETDuet-1 harboring *glmU* from *E. coli* K-12 MG1655 (DE3)	This study
pETDuet_sodA_glmU	pETDuet-1 harboring *sodA* and *glmU*	This study
pCDFDuet_mltB	pCDFDuet-1 harboring *mltB* from *E. coli* K-12 MG1655 (DE3)	This study
pCRISPath_ybiV	pCRISPathBrick harboring protospacer to target *ybiV* for underexpression	This study

This journal is © The Royal Society of Chemistry and IChemE 2024

Mol. Syst. Des. Eng., 2024, **9**, 597–611 | **599**

acetylglucosaminidase (nagZ) deletion. *mltB*, *sodA* and *glmU* have been amplified from *E. coli* K-12 MG1655 (DE3) genome and cloned using the primers glmU_Fw, glmU_Rv, sodA_Fw, sodA_Rv, mltB_Fw and mltB_Rv (Table S1†) under the same conditions as previously described for chondroitin pathway construction. pETDuet-1 was used as a vector to overexpress *glmU* and/or *sodA*, while overexpression of *mltB* was conducted using pCDFDuet-1 as an expression vector. pCRISPathBrick plasmid (Table 1) was used to implement the CRISPR interference (CRISPRi) system, by expressing and targeting a dCas9 (dead Cas9).[47] The protospacer for *ybiV* and *murJ* targeting was inserted using Golden Gate assembly. For this procedure, annealing of pairs of oligos (ybiV_UE_Fw, ybiV_UE_Rv for *ybiV*, Table S1,† and murJ_UE_Fw, murJ_UE_Rv or murJ2_Fw, murJ2_Rv for *murJ*, Table S2†) has been conducted by incubating 100 μmol of each oligo in T4 DNA ligase buffer at 95 °C for 5 min and letting the temperature slowly decrease until room temperature was reached. Then the annealed oligo was mixed with the plasmid pCRISPathBrick, *Bsa*I (= *Eco*31I) and T4 DNA ligase. The mixture was incubated through 10 cycles of 5 min at 37 °C and 10 min at 22 °C, followed by 30 min at 37 °C and 15 min at 75 °C. All constructed plasmids were verified by colony PCR, digestion and their sequences were further confirmed by sequencing.

In the attempts to delete *nagZ* gene, the protocol for gene deletion using a CRISPR-Cas9 strategy was followed.[48] The primers used are described in Table S2.†

Flask fermentations

For chondroitin screening production tests in conical flask fermentations, *E. coli* K-12 MG1655 (DE3) and *E. coli* BL21 (DE3) harboring the heterologous chondroitin production pathway (pRSFDuet_kfoCA_Zmugd) have been used. Also, variations of these strains, with over and/or underexpression of genes, have been evaluated.

Flasks of 250 mL with 50 mL lysogeny broth (LB) Miller (NZYTech) supplemented with suitable antibiotics (*i.e.*, depending on the plasmid(s) present in the strain, 50 μg mL^{-1} of kanamycin (Fisher), 100 μg mL^{-1} of ampicillin (Fisher Bioreagents), 100 μg mL^{-1} of spectinomycin (Alfa Aesar) and/or 34 μg mL^{-1} chloramphenicol (Alfa Aesar)) have been inoculated with 1% (v/v) of an overnight culture. The cultures were incubated at 37 °C and 200 rpm until OD$_{600nm}$ of 0.6–0.8 was reached. At this point, isopropyl β-D-1-thiogalactopyranoside (IPTG, 1 mM; NZYTech) was added to induce heterologous enzyme production and temperature was decreased to 30 °C. The cultures were further incubated for 24 h. All assays were conducted in triplicate.

Bioreactor operation

The engineered *E. coli* K-12 MG1655 (DE3) strains were collected from LB plates supplemented with suitable antibiotics and used to inoculate pre-inoculums of 10 mL of LB medium. The cultures were grown at 37 °C and 200 rpm for about 22 h. Cells were harvested by centrifugation (4000 × *g*, 15 min) and used to inoculate 500 mL conical flasks containing 120 mL of defined medium (per liter: yeast extract 2 g (Labkem, Baldoyle, Ireland), K$_2$HPO$_4$ 10 g (Panreac, Barcelona, Spain), KH$_2$PO$_4$ 2 g (Panreac), MgCl$_2$ 0.1 g (VWR, Radnor, USA), sodium citrate 0.5 g (Panreac), (NH$_4$)$_2$SO$_4$ 1 g (Labkem), and glucose 20 g (Acros Organics, Geel, Belgium)) (second pre inoculum) which were then shaken at 200 rpm and 37 °C for about 16 h, and used to inoculate the bioreactor with an initial OD$_{600nm}$ of 0.1. Fermentations were performed in a 2-L DASGIP® Parallel Bioreactor System (Eppendorf, Hamburg, Germany). The operating volume for the fermentation was 400 mL of defined medium and suitable antibiotics. The temperature set-point was maintained at 37 °C, and the pH was automatically controlled at 7 by addition of 2 M NaOH (Sigma, St. Louis, USA). The dissolved oxygen was kept above 30% of saturation by using stirring-speed feedback-control ranging from 250 rpm until 800 rpm and a constant air-flow rate of 0.5 volume air per volume medium per min (12 L h^{-1}).

After 3 h (OD$_{600nm}$ ~0.6), 1 mM IPTG was added to the culture and temperature was reduced to 30 °C. The fermentation continued until glucose was completely consumed (until ~54 h). Samples were taken during the fermentation to monitor glucose concentration and OD$_{600nm}$.

For fed-batch fermentations, the batch phase was performed as previously described except that the initial glucose concentration was 10 g L^{-1}. When glucose concentrations were reduced up to 2–3 g L^{-1}, the feeding phase was initiated by feeding a concentrated solution (80 g L^{-1} glucose and 18 g L^{-1} yeast extract) with a constant feeding rate of 1.5–2.5 mL h^{-1}, depending on the glucose consumption rate of the strain. All fermentations were conducted in duplicate.

Analytic methods

Samples from *E. coli* fermentations were centrifuged to separate cells from the supernatant (4000 × *g*, 15 min).

The supernatants from the end of flask fermentations were used to quantify extracellular chondroitin while the pellets were further processed to determine intracellular chondroitin.

Pellets (from ~50 mL of culture) were washed and then resuspended in deionized water (5 mL). The suspended cells were lysed by sonication with a microtip probe linked to Vibra-cell processor (Sonics, Newtown, CT, USA). Keeping the solution on ice during the procedure, short pulses of 3 s ON and 4 s OFF at 30% amplitude were performed until 5 min of active sonication was reached. The resulting lysate was centrifuged (12 000 × *g* 15 min) to remove the insoluble material.

For intracellular chondroitin quantification, the lysates were treated with DNase (New England Biolabs, MA, USA) for 2 h at 37 °C and then with proteinase K at a final

concentration of 2 mg mL^{-1} (NZYTech) for 2 h at 56 °C. Then, the mixture was boiled for 5 min and centrifuged again (16 000 × g 20 min) to remove the insoluble material.

Both extracellular and intracellular samples were precipitated by adding three volumes of cold ethanol and letting the mixture at 4 °C overnight. The precipitate was collected by centrifugation at 4000 × g for 10 min at 4 °C. The precipitate was air-dried at room temperature overnight after which it was resuspended in deionized water. The insoluble material was removed by centrifugation (16 000 × g for 20 min). Chondroitin was quantified by the uronic acid carbazole assay[50] using chondroitin sulfate (Biosynth, Staad, Switzerland) solutions as standards. Samples or standards (125 μL) were mixed with 750 μL sulfuric acid reagent (9.5 g L^{-1} sodium tetraborate, Supelco, Bellefonte, USA, dissolved in H$_2$SO$_4$ > 95%). The mixture was boiled for 20 min. Afterwards, 25 μL of carbazole reagent (1.25 g L^{-1} carbazole, Supelco, dissolved in absolute ethanol, Fisher) were added to the boiled samples. The mixture was boiled again for 15 min and cooled down for 15 min. The OD$_{530nm}$ was then read in a microplate reader.

Protein expression in cultured *E. coli* K-12 MG1655 (DE3) carrying pETDuet-1, pETDuet_glmU, pETDuet_sodA, pCDFDuet-1, or pCDFDuet_mltB, was evaluated by sodium dodecyl sulfate polyacrylamide gel electrophoresis (SDS-PAGE)[46] (4% stacking gel and 12% running gel). Samples (soluble and insoluble fractions of lysates) were mixed with 2× Laemmli sample buffer (65.8 mM Tris–HCl pH 6.8, 2.1% SDS, 26.3% glycerol, 0.01% bromophenol blue and 5% β-mercaptoethanol, from Fisher Scientific, JMGS, Sigma-Aldrich and AppliChem, respectively) and denatured at 95 °C for 5 min. The protein marker used was Color Protein Standard—Broad Range (NEB, #77125). After electrophoresis, the gel was stained using Coomassie Blue R-250 (AppliChem) for 15 min and de-stained using distilled water.

Samples from bioreactors were collected along the fermentations and analyzed in terms of glucose consumption and cellular growth. Final extracellular chondroitin was quantified using the carbazole method described above. Glucose consumption was monitored along the fermentations through the dinitrosalicylic acid (DNS) method.[51] 3,5-Dinitrosalicylic acid (Acros Organics), sodium potassium tartrate tetrahydrate (Panreac) and NaOH (Sigma) were used to prepare the DNS reagent, which was mixed with the same volume of samples, boiled and cooled down by adding deionized water. The OD$_{540nm}$ was then measured. The glucose concentrations were further confirmed by high performance liquid chromatography (HPLC) using a JASCO system associated with a refractive index (RI) detector (RI-2031), and an Aminex HPX-87H column from Bio-Rad, which was kept at 60 °C; the mobile phase used was 5 mM H$_2$SO$_4$ (Fisher) at a flow rate of 0.5 mL min^{-1}. All ODs were measured in a 96-well plate spectrophotometric reader Synergy HT (BioTek, Winooski, VT, USA), to establish the growth profile.

Results and discussion

Bioinformatic results for mutant prediction

OptFlux was used to identify potential *E. coli* mutants with enhanced capabilities to produce increased quantities of chondroitin. Using this tool, it was not possible to predict the improvement of chondroitin production by combining gene knockouts (*data not shown*). This was likely because the competing pathways that use the intermediates are critical for cell growth. However, performing gene over- and underexpression searches allowed the identification of several possible targets. Table S3† displays the genetic modifications identified as potential phenotypes with the highest BPCY for each model.

Most of the resulting solutions comprised two combined modifications, namely underexpression of one of the genes from cell wall biosynthesis and recycling pathways (such as: lytic transglycosylases MltABCEF and Slt; anhydromuropeptide permease AmpG; oligopeptide permeases *oppBCDF*; or *N*-acetylmuramoyl L-alanine amidases AmiABC) and overexpression of one of the genes responsible for the production of a chondroitin precursor (either glucosamine-1-phosphate *N*-acetyltransferase/UDP-*N*-acetylglucosamine diphosphorylase GlmU or phosphoglucosamine mutase GlmM). Underexpression of cytidylate kinase *cmk* and UMP kinase *pyrH* genes was also identified, which catalyze reactions from the biosynthesis and salvage of pyrimidine ribonucleotides (Fig. 1).

Overexpressions of *glmM* and/or *glmU* are well reported metabolic engineering strategies for improving the production of chondroitin[52] or hyaluronic acid[53] in *E. coli*.

In Gram-negative bacteria, the cell-wall recycling is initiated in the periplasm by bacterial lytic transglycosylases such as Slt and MltABCEF, which degrade murein (peptidoglycan), the major cell wall component, at the glycosidic bond between *N*-acetylglucosamine (GlcNAc) and *N*-acetylmuramic acid (MurNAc), releasing a distinctive 1,6-anhydro-*N*-acetyl-β-D-muramyl (AnhydroMurNAc) product. The anhydromuropeptide permease AmpG specifically transports the resulting AnhydroMurNAc-containing muropeptides, from the periplasm into the cytoplasm.[54–56] MurNAc-L-Ala amidases, AmiABC, are another class of peptidoglycan degrading enzymes in the periplasm that cleave the amide bond between MurNAc and the stem peptide in peptidoglycan, releasing murein tri-, tetra-, and pentapeptides into the periplasm from which they diffuse out of the cell, or enter the cytoplasm *via* the MppA-OppBCDF permease system.[57] The membrane oligopeptide permeases OppBCDF and the murein tripeptide ABC transporter periplasmic binding protein MppA constitute an ABC transporter which is involved in the recycling of the murein tripeptide from either exogenous sources or from amidase action.[57,58] Once in the cytoplasm, the muropeptides are degraded by amidase AmpD, β-*N*-acetylglucosaminidase NagZ, and LD-carboxypeptidase LdcA, and their constituent components are used for lipid II biosynthesis. The lipid II
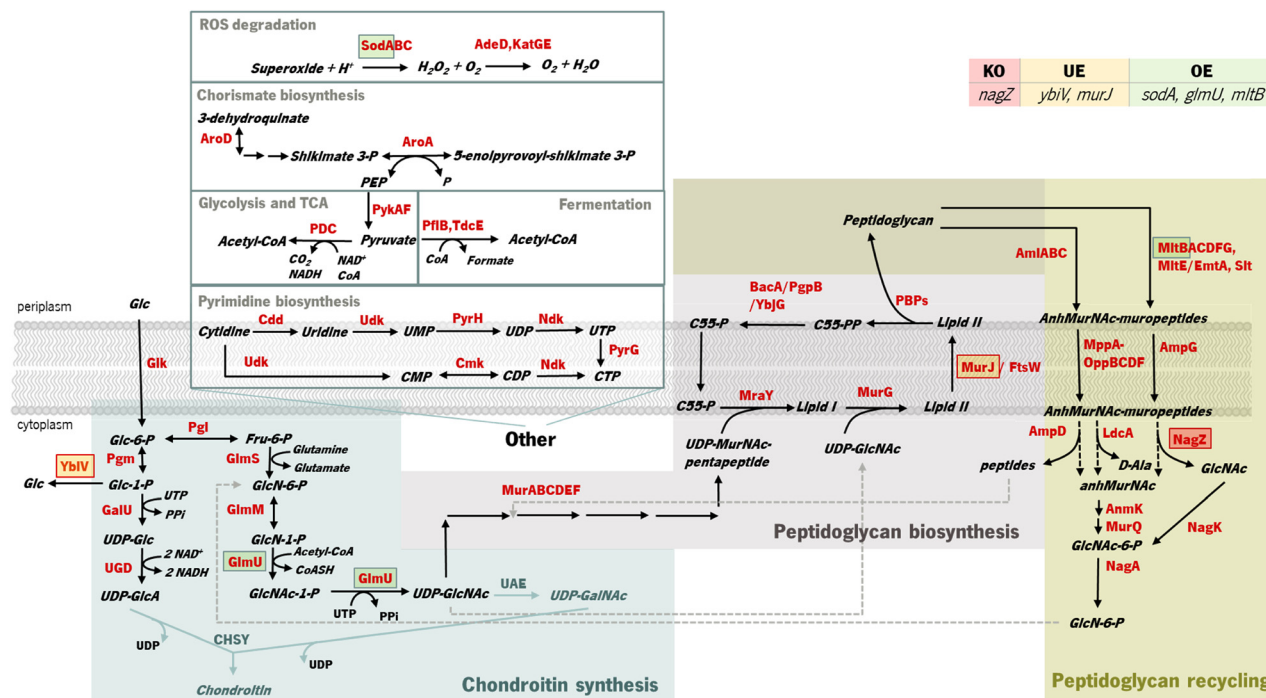
This journal is © The Royal Society of Chemistry and IChemE 2024

Mol. Syst. Des. Eng., 2024, **9**, 597–611 | **601**

Fig. 1 Identified targets for genetic modification to potentially improve chondroitin heterologous production in *Escherichia coli* and their role in bacterial metabolism. The target for knock-out (KO) is marked in a red square, underexpressions (UE) are marked in orange squares, and overexpressions (OE) are marked in green squares. MltB, MurJ and NagZ are involved in cell wall biosynthesis and recycling, while GlmU produces the chondroitin precursor uridine-diphosphate (UDP)-*N*-acetylglucosamine and YbiV dephosphorylates the precursor glucose 1-phosphate. SodA is not directly related to the metabolism of chondroitin synthesis intermediates. Enzyme and compound abbreviations: AdeD: adenine deaminase; AmiABC and AmpD: *N*-acetylmuramoyl-ʟ-alanine amidases; AmpG: anhydromuropeptide permease; AnmK: anhydro-*N*-acetylmuramic acid kinase; AroA: 3-phosphoshikimate 1-carboxyvinyltransferase; BacA: undecaprenyl pyrophosphate phosphatase; C55: di-*trans,octa-cis*-undecaprenyl; Cdd: cytidine/deoxycytidine deaminase; CHSY: chondroitin synthase; Cmk: cytidylate kinase; FtsW: peptidoglycan glycosyltransferase; GalU: uridine-triphosphate(UTP): glucose-1-phosphate uridylyltransferase; Glk: glucokinase; GlmU: glucosamine-1-phosphate *N*-acetyltransferase/UDP-*N*-acetylglucosamine diphosphorylase; GlmM: phosphoglucosamine mutase; GlmS: glucosamine-6-phosphate synthase; KatGE: catalases; LdcA: murein tetrapeptide carboxypeptidase; MltABCDFG: membrane bound lytic transglycosylases; MppA-OppBCDF: oligopeptide permeases complex with muropeptide-binding protein; MraY: phospho-*N*-acetylmuramoyl-pentapeptide-transferase; MurG: *N*-acetylglucosaminyl transferase; MurJ: lipid II flippase; MurQ: *N*-acetylmuramic acid 6-phosphate etherase; NagA: *N*-acetylglucosamine-6-phosphate deacetylase; NagK: *N*-acetyl-ᴅ-glucosamine kinase; NagZ: β-*N*-acetylglucosaminidase; Ndk: nucleoside diphosphate kinase; PBPs: penicillin-binding proteins; PDC: pyruvate dehydrogenase complex encoded by genes *pdhA*, *pdhB* and *lpd*; PflB: pyruvate formate-lyase; Pgi: glucose-6-phosphate isomerase; Pgm: phosphoglucomutase; PgpB: phosphatidylglycerophosphatase B; PykAF: pyruvate kinases; PyrG: CTP synthetase; PyrH: UMP kinase; Slt: soluble lytic transglycosylase; SodA: superoxide dismutase; TdcE: 2-ketobutyrate formate-lyase/pyruvate formate-lyase 4; UAE: UDP-*N*-acetylglucosamine 4-epimerase; Udk: uridine/cytidine kinase; UGD: UDP-glucose 6-dehydrogenase; YbjG: undecaprenyl pyrophosphate phosphatase; YbiV: sugar phosphatase.

assembled in the cytoplasm is delivered to the periplasm for the *de novo* synthesis of peptidoglycan.[56] Consequently, peptidoglycan biosynthesis is the main competing pathway that redirects precursors from chondroitin biosynthesis. Although these reactions result in the production of the chondroitin precursor glucosamine 6-phosphate (GlcN-6-P) that can also be produced by glucose, they consume the intermediate UDP-acetylglucosamine (UDP-GlcNAc) (Fig. 1). Therefore, underexpressing cell wall recycling pathway genes might lead to more available precursors, as predicted by the models.

The pyrimidine nucleotide metabolic process was also identified as a target pathway to be modified to increase chondroitin production. Cmk rephosphorylates cytidylate (CMP) and deoxycytidylate (dCMP). Underexpression of *cmk* (included in an optimization solution using iB21_1397_c

model) could lead to an improved uridine-5′-triphosphate (UTP) pool as observed in a *cmk* deletion mutant.[59] This is beneficial for chondroitin production because UTP is a co-factor in chondroitin-precursor biosynthesis steps catalyzed by GalU and GlmU. Uridine monophosphate (UMP) kinase PyrH is also involved in the biosynthesis of pyrimidine nucleotides, specifically catalyzing the phosphorylation of UMP to UDP. In this case, targeting this gene for underexpression, as obtained in an optimization solution using the iB21_1397_c model, has no obvious explanation and no literature was found to support that the underexpression of *pyrH* would improve the UTP pool, or in other manner be directly beneficial for chondroitin biosynthesis. However, unexpected targets can have other mechanisms for improving product titers. Targeting genes from purine and pyrimidine biosynthesis pathways for

underexpression (including *cmk* and *pyrH*) has been applied for antibody production[60] as a growth decoupling strategy to increase product formation. Inhibiting excess biomass formation allows for carbon to be utilized efficiently for product formation instead of growth, resulting in increased product yields and titers.[60] Interestingly, in Landberg *et al.* (2020)[60] study, from the reported 21 selected targets for underexpression, repression of *cmk* consistently resulted in higher product titers. On the other hand, *pyrH* underexpression did not affect production. It is also relevant to mention that the models herein used are stoichiometric models, therefore, they do not comprehend kinetic information that would be valuable for this analysis. The model iB21_1397_c has the UMP kinase reaction set as reversible and as being catalyzed by both *pyrH* and *cmk* encoded enzymes, although it is known that the specific favored reactions are, *in vivo*, the phosphorylation of UMP and phosphorylation of CMP (or dCMP), respectively.[61,62] Also, *pyrH* is a known essential gene for *E. coli* growth.[63] Therefore, although *pyrH* has been identified *in silico* as a target for underexpression, this might not be the best target for improving chondroitin production.

Generally, solutions herein obtained with different models were composed by similar genetic modifications demonstrating the robustness of the modifications associated with the overproduction of chondroitin. Despite allowing for a maximum of 10 modifications, the solution comprised usually only two genetic modifications (the highest number of modifications was five with model iECBD_1354_c, Table S3†), thus suggesting that the solutions can be further improved using other approaches.

The FVA analysis shows the range of flux distributions of chondroitin. To evaluate the robustness of a solution, the difference between the minimum and maximum chondroitin production, for a fixed biomass value, should be minimal. The solutions that included oligopeptide permease *oppBCDF* gene underexpression (iEC1356_Bl21DE3_c, Table S3†) resulted in a greater difference between minimum and

maximum chondroitin production, suggesting that they are less robust.

To seek for more robust mutants, a different computational approach was performed using MEWpy.[39] Using this approach, instead of maximizing one objective function (BPCY), two objective functions were defined, namely the BPCY and WYIELD, which allow guidance of the evolutionary algorithm onto more robust solutions. BPCY was calculated by MEWpy by multiplying the biomass by product, based on pFBA predictions. WYIELD is the weighed sum of the minimum and maximum product fluxes, constrained to a fixed growth.

Since the model iB21_1397_c achieved the best optimization results (highest BPCY of 0.09607 and highest chondroitin flux of 2.6168 mol gDW^{-1} h^{-1}), when using OptFlux, this model was selected to be used in MEWpy. The same environmental conditions were set, and the evolutionary optimization was run. This procedure resulted in 76 solutions, with 39 identified targets for genetic modification. The type and frequency of each genetic modification throughout all solutions are analyzed in Fig. 2.

The results from the best solutions obtained using MEWpy are shown in Table 2. Solutions 1 and 2 have the highest BPCY score, while solutions 5, 6 and 7 exhibited the highest WYIELD. Phenotype simulation was then performed using OptFlux, with pFBA as a simulation method, for each solution and the results are also shown in Table 2.

The MEWpy method allowed identification of new mutants with improved chondroitin production, as high as 2.9150 mol gDW^{-1} h^{-1}, while the highest production obtained from OptFlux solutions was 2.6168 mol gDW^{-1} h^{-1} (Table S3†).

As occurred in the optimization results obtained using OptFlux, solutions from MEWpy included targets from peptidoglycan biosynthesis and recycling pathways (*nagZ*, *murJ*, *mltB*) and the pyrimidine ribonucleotide salvage pathway (*cmk*). Maltodextrin glucosidase (*malZ*) releases
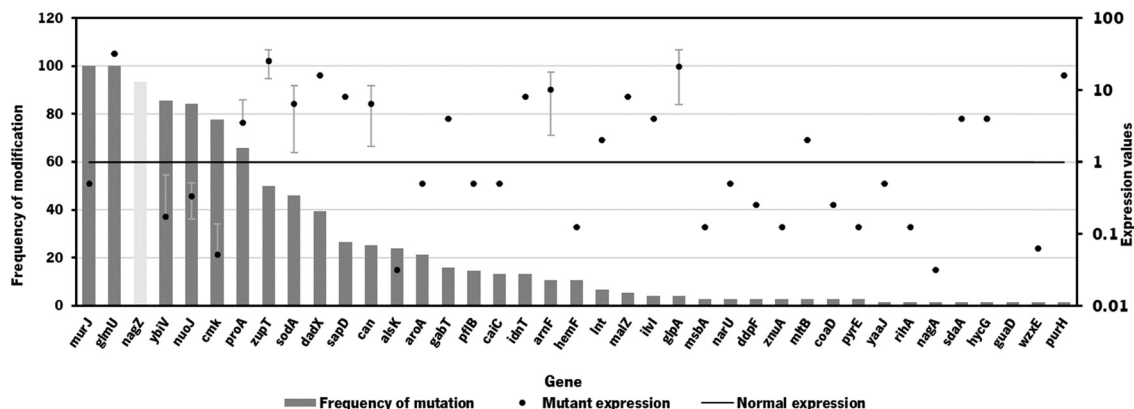

Fig. 2 Frequency of genetic modifications in the 76 solutions from strain optimization using the MEWpy tool. The mutant expression (in dots) represents the average expression value. Mutant expressions higher than 1 represent overexpression while values of expression lower than 1 represent underexpression. Deletions are represented in light grey bars.

Table 2 Optimization results obtained for the iB21_1397_c model using the MEWpy tool in Python, and the corresponding relevant fluxes according to phenotype simulations using parsimonious flux balance analysis (FBA) in OptFlux. BPCY was calculated by multiplying the biomass by product and then dividing by the substrate consumed, as predicted by pFBA. WYIELD is the weighed sum of the minimum and maximum product fluxes. Flux variability analysis (FVA) results are shown as minimum and maximum chondroitin obtained for fixed biomass. Predicted biomass and chondroitin values are in units of h^{-1} and mmol gDW^{-1} h^{-1}, respectively

			Genes modified			Predicted phenotype (pFBA)		FVA	
Solution	BPCY	WYIELD	Knock-out	Under expression	Over expression	Biomass	Chondroitin	Min chondroitin	Max chondroitin
1	0.08840	2.91104	nagZ	ybiV, alsK, aroA, pflB, murJ, narU	sodA, glmU, mltB	0.3040	2.9079	2.9034	2.9289
2	0.08887	2.90887	ybiV	alsK, aroA, murJ, proA	idnT, lnt, glmU, gabT, malZ	0.3056	2.9079	2.9033	2.9220
3	0.04316	3.14641	nagZ, ybiV	pflB, murJ, msbA, cmk	sodA, sapD, glmU	0.1221	2.9150	2.9150	3.6863
4	0.04316	3.14651	nagZ	ybiV, pflB, murJ, msbA	sodA, sapD, idnT, glmU	0.1221	2.9150	2.9150	3.6866
6	0.04340	2.95361	nagZ	ybiV, alsk, aroA, murJ, pyrE	sodA, glmU, zupT, mltB	0.1221	2.9354	2.6382	3.6896
Selected genes	0.08840	2.91104	nagZ	ybiV, murJ	sodA, glmU, mltB	0.3040	2.9079	2.9034	2.9289

glucose from malto-oligosaccharides as part of the glycogen degradation pathway,[64] and its suggested overexpression might be to improve glucose and glucose 6-phosphate availability through recycling of those carbon stocks. Many of these new solutions included varied transporters (narU, znuA, sapD, msbA, idnT) that were not found to be related to chondroitin production. Other genes that were not found to be related to the chondroitin biosynthesis pathway, co-factor production or competing pathways were: D-allose kinase alsK that catalyzes the phosphorylation of D-allose to D-allose 6-phosphate; aroA that encodes 3-phosphoshikimate 1-carboxyvinyltransferase which is involved in the chorismate pathway, leading to aromatic amino acid biosynthesis; enzyme apolipoprotein N-acyltransferase (lnt) that transfers a fatty acid from phospholipid to the amino terminus of a diacylglycerol prolipoprotein as part of the lipoprotein posttranslational modification pathway; purH that encodes the bifunctional phosphoribosylaminoimidazolecarboxamide formyltransferase/inosinic acid cyclohydrolase involved in the de novo biosynthesis of purine nucleotides; glutamate-5-semialdehyde dehydrogenase encoded by proA that is from the L-proline biosynthesis; 4-aminobutyrate aminotransferase GabT that is involved in 4-aminobutyrate (GABA) degradation.

Overexpression of glmU, responsible for producing a chondroitin precursor UDP-GlcNAc, was included in most solutions, as occurred in those resulting from OptFlux.

Gene nagZ encodes β-N-acetylglucosaminidase (NagZ), an enzyme involved in peptidoglycan recycling. NagZ acts specifically by hydrolyzing the β-1,4 glycosidic bond, removing N-acetyl-glucosamine (GlcNAc) residues from peptidoglycan fragments that have been excised from the cell wall during growth.[65] Gene murJ encodes for lipid II flippase (MurJ) which flips lipid II from the inner face of the inner membrane to the outer face, being essential for peptidoglycan polymerization.

The gene mltB, described above, was identified, in the best solution from MEWpy, as a target for slight overexpression (expression value: 2), contrary to the solutions obtained in OptFlux, where it has been suggested for underexpression. This might be related to the combination and number of genes being different in the solutions, and mltB overexpression might be required to compensate for the negative effect on growth, caused by changes in the expression of several genes. The sugar phosphatase YbiV has been indicated in most solutions for either underexpression or knockout. This is a logical solution as this enzyme redirects metabolic flux from chondroitin production by phosphating glucose-6-phosphate into glucose[66] (Fig. 1). Pyruvate formate-lyase encoded by pflB, which catalyzes non-oxidative cleavage of pyruvate to acetyl-CoA and formate in anaerobically growing cells, was included in some solutions (14%) as underexpressed. The underexpression of pflB would decrease the flux through this reaction, leading to an increased availability of pyruvate, and consequently improved glucose-6-phosphate or fructose-6-phosphate levels. In fact, pflB deletion has been a common reported target for increased dicarboxylic acid production.[67–69]

Another common gene identified for overexpression was the superoxide dismutase sodA. This gene is expressed in response to oxidative stress and acts by destructing toxic superoxide radicals that are naturally produced during respiratory growth.[70] No direct relationship with chondroitin production improvement was found.

Based on genetic modification frequency, and after confirming that the phenotypes did not vary much from the originally proposed solution (Table 2), the gene selection was narrowed, from genes present in the best solution (solution 1), for genes with more potential to engineer efficient E. coli strains. These selected modifications were: nagZ deletion,
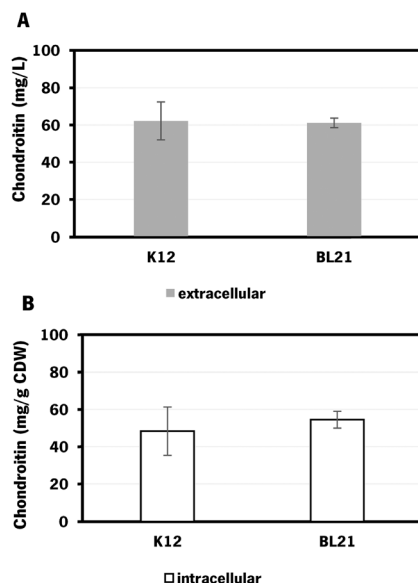
Fig. 3 Chondroitin production in *Escherichia coli* engineered strains with chondroitin biosynthetic pathway in flask fermentation: A – extracellular chondroitin in mg L^{-1} and B – intracellular chondroitin in mg g^{-1} CDW, using K12 – *E. coli* K-12 MG1655 (DE3) and BL21 – *E. coli* BL21 (DE3), both carrying pRSFDuet_kfoCA_Zmugd. Assays were performed in triplicate. CDW – cell dry weight.

ybiV and *murJ* underexpressions and *sodA*, *glmU* and *mltB* overexpressions. A schematic representation of the affected pathways with these genetic modifications is presented in Fig. 1.

The individual modifications and cumulative modifications of the selected genes were experimentally implemented, to study which gene combinations could benefit chondroitin production the most without compromising *E. coli* growth.

In vivo validation of bioinformatic results

Chondroitin production using engineered *E. coli*. The biosynthetic pathway for heterologous production of chondroitin was constructed by cloning the genes *kfoC* and *kfoA* from *E. coli* O5:K4:H4 and *Zmugd* in the plasmid pRSFDuet-1. The amplification products are shown in Fig. S1.† The assembled pathway was expressed in both *E. coli* K-12 MG1655 (DE3) and *E. coli* BL21 (DE3) to evaluate chondroitin production (Fig. 3).

E. coli K-12 harboring the biosynthetic pathway for chondroitin production was able to produce 62 ± 10 mg L^{-1} of extracellular chondroitin and 48 mg g^{-1} of cell dry weight (CDW) of intracellular chondroitin. *E. coli* BL21 was able to produce 61 ± 3 mg L^{-1} of extracellular chondroitin and 55 mg g^{-1} CDW of intracellular chondroitin. These results are higher than the ones obtained in a recent work[71] that reported a production of intracellular sulfated chondroitin of 126.64 μg g^{-1} CDW and 13.14 μg g^{-1} CDW using *E. coli* O5:K4:H4 and *E. coli* K-12 MG1655, respectively, in flasks. These strains harbored a biosynthetic pathway for chondroitin production comparable to the one herein used (*kfoC*, *kfoA* and *kfoF*, naturally present in *E. coli* O5:K4:H4), but also expressed a chondroitin-4-*O*-sulfotransferase and lacked PAPS reductase *cysH* for the sulfation of chondroitin.

Extracellular chondroitin is more commonly measured, possibly because of its ease of purification and quantification, which makes it of greater interest for biotechnological production. Extracellular chondroitin production using engineered *E. coli* in shake flask cultivation has been reported to achieve concentrations of up to 213 mg L^{-1} (Table 3) while chondroitin-derived compounds have reached concentrations of up to 1739 mg L^{-1},[36,71–75] depending on the host, biosynthetic pathway, chassis optimizations and culture conditions.

Table 3 Selected studies on chondroitin production in different hosts using genetic engineering approaches. For a more extensive review of microbial production of other chondroitin-derived glycosaminoglycans please see[31]

Host	Substrate	Genetic modification	Operational mode	Titer (mg L^{-1})	Ref.
Escherichia coli O10:K5:H4	Glucose	*kfoC* and *kfoA* expression overexpression	Shake-flask	52.6	76
E. coli BL21 Star (DE3)	Glucose	*kfoC*, *kfoA* and *kfoF* expression in pseudo-operon gene configuration	Flask / Bioreactor (fed-batch)	213 / 2400	36
Streptococcus equi subsp. *zooepidemicus*	Sucrose	*kfoC* and *kfoA* expression overexpression	Flask / Bioreactor (batch)	90 / 300	77
Bacillus subtilis 168	Sucrose	*kfoC*, *kfoA*, and *tuaD* overexpression	Flask / Bioreactor (fed-batch)	2540 / 5220	43
Corynebacterium glutamicum	Glucose	Native *kfoC*, *kfoA* and *ugdA* overexpression; Δ*ldh*	Bioreactor (fed-batch)	1910	78
Pichia pastoris	Methanol	*kfoC*, *kfoA* and *tuaD* overexpression	Flask	189.8	79
E. coli K-12 MG1655 (DE3)	Glucose	*kfoC*, *kfoA* and *ugd* overexpression	Flask / Bioreactor (batch) / Bioreactor (fed-batch)	62 / 300 / 621	This study
E. coli K-12 MG1655 (DE3)	Glucose	*kfoC*, *kfoA*, *ugd* and *mtlB* overexpression	Flask / Bioreactor (batch) / Bioreactor (fed-batch)	91 / 427 / 535	This study

The highest chondroitin titers reported have been obtained using engineered *E. coli* O5:K4:H4, which naturally produces a fructosylated chondroitin, in defined medium, and in batch or fed-batch fermentations in bioreactors. For instance, a three-phase fermentation with pathogenic *E. coli* O5:K4:H4 overexpressing gene from transcription antitermination protein *rfaH* led to 9.2 g L^{-1} of chondroitin using glucose as a substrate, and in a larger scale, the same strain produced 9 g L^{-1} using glycerol as a substrate.[72] To avoid the risks of using pathogenic bacteria, there have been efforts to construct alternative hosts to be efficient for chondroitin production using metabolic engineering strategies. A *Bacillus subtilis* 168, overexpressing *kfoC* and *kfoA* from *E. coli* K4 and *tuaD* (UDP-glucose 6-dehydrogenase) from *B. subtilis*, growing on sucrose, has achieved 5.22 g L^{-1} of chondroitin in fed-batch fermentation.[43]

As the culture medium herein used for these initial screening tests in flasks was LB, the optimal production of chondroitin could be further optimized using different culture conditions. Based on work with the highest reported chondroitin production,[72] a defined medium was used for further fermentations in a bioreactor.

As the difference in chondroitin production between the two hosts was not significant (Fig. 3), the *E. coli* K-12 MG1655 (DE3) was selected for further engineering strategies. This strain is recognized for its enhanced genetic manipulability compared to *E. coli* BL21 (DE3).[80]

Construction of engineered *E. coli* strains based in bioinformatics optimization. Based on the bioinformatics results, the selected modifications to be implemented towards an enhancement of chondroitin production were the overexpression of *sodA*, *glmU* and *mltB*; the deletion of *nagZ*; and the underexpression of *ybiV* and *murJ*. The genes *sodA*, *glmU* and *mltB* for overexpressions were amplified (Fig. S2A†) and cloned in pETDuet-1 or pCDFDuet-1. The plasmid with lower copy number (pCDFDuet-1) was used for *mltB* since, from the overexpressions predicted, it was the one with lower expression value (Fig. 2). Their expression was confirmed by SDS-PAGE (Fig. S2B†).

The *nagZ* knockout was attempted multiple times in *E. coli* K-12 MG1655 (and afterwards in *E. coli* BL21) using a CRISPR-Cas9 strategy[48] (schematized on Fig. S3†), but it was unsuccessful. The primers used for this strategy are described in Table S2.† Although this gene is reported as non-essential for *E. coli* growth and has been previously deleted[81] using a different recombination-based strategy,[82] it has a described role in cell wall biosynthesis as was previously mentioned. Therefore, it is possible that a strain lacking *nagZ* could be more susceptible to the antibiotics used as selective markers in the attempted CRISPR-Cas9 strategy (spectinomycin and chloramphenicol). A deletion of this gene could affect the cell wall integrity or permeability, that is maintained by the coordinated and regulated action of enzymes involved in the peptidoglycan synthesis and recycling.[83] In fact, the improved sensibility to β-lactam antibiotics in Gram-negative strains lacking *nagZ* compared

to wild-type strains has been widely reported.[65,83,84] If the cells are more susceptible to the antibiotics used in the selection medium, then it could affect the growth and survival of the cells during the gene editing process. The selective pressure applied by the antibiotics could be too strong, resulting in a decrease in the number of cells that survive and grow on the selection medium. One possible solution to this issue could be to use lower concentrations of the antibiotics to reduce the effect on growth of cells lacking *nagZ*. The integration of the chondroitin pathway genes in the genome without maintenance of antibiotic resistance markers can also be an efficient strategy to reduce the toxic effect of antibiotics.

Regarding gene underexpressions, a CRISPRi system[47] was designed and constructed. In this strategy, a modified version of the caspase 9 protein commonly called as dead Cas9 (dCas9), which does not have nuclease activity but maintains sequence-specific double stranded DNA-binding capability, is expressed to target the gene, ultimately repressing its expression. The CRISPRi system for *ybiV* underexpression was successfully constructed and evaluated. However, underexpression of *murJ* was not evaluated because construction of targeting protospacer has failed. A schematic representation of the strategy used can be found in Fig. S3.† The primers used in the attempts of constructing the protospacer for *murJ* underexpression are described in Table S2.†
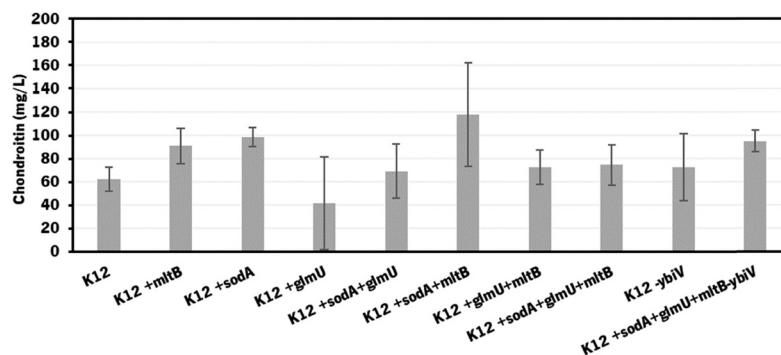
The individual and cumulative genetic modifications (*sodA*, *glmU*, and *mltB* overexpressions and/or *ybiV* underexpression) were further evaluated *in vivo*.

Chondroitin production in shake flasks using *E. coli* engineering strains based in bioinformatic optimizations. The solutions obtained though bioinformatics were further validated *in vivo*. Each modification was individually evaluated in the engineered *E. coli* strain harboring the chondroitin pathway already expressing 3 heterologous genes (*kfoC*, *kfoA* and *Zmugd*), through shake flask fermentations (Fig. 4) to seek for mutants with improved chondroitin production carrying as few modifications as possible.

In these screening shake flask experiments, *E. coli* K-12 mutants were able to produce extracellular chondroitin from 42 to 118 mg L^{-1}. Even though the differences in chondroitin production were not significant (*p*-value > 0.05), mutants overexpressing *sodA* or *mltB*, or the one overexpressing both these two genes, seemed to be the most promising ones. As the cumulative effect of both overexpressions was not significantly better than the individual mutations, the two mutants containing individually overexpressed *sodA* or *mltB* were selected for further scale-up studies, in a more suitable culture medium for chondroitin production.

Chondroitin production in bioreactor (batch experiments). The two selected mutant strains were cultured at the bioreactor scale, in batch mode, starting with 20 g L^{-1} of glucose. The performance of both strains was further

	K12	K12 +mltB	K12 +sodA	K12 +glmU	K12 +sodA +glmU	K12 +sodA +mltB	K12 +glmU +mltB	K12 +sodA +glmU +mltB	K12 -ybiV	K12 +sodA +glmU +mltB -ybiV
Yield chondroitin/ biomass (mg/g CDW)	119 ±6	142 ±45	299 ±38	70 ±70	161 ±48	412 ±163	207 ±41	233 ±50	140 ±40	224 ±41

Fig. 4 Chondroitin production in *E. coli* K-12 MG1655 harboring the chondroitin biosynthetic pathway (K12, genes *kfoC*, *kfoA* and *Zmugd*) with additional modifications: *sodA*, *glmU* and *mltB* overexpressions and/or *ybiV* underexpression. The table shows a comparison of chondroitin yield related to cell dry weight (CDW), obtained for the different mutants.

compared to the control (*E. coli* K-12 harboring pRSFDuet_kfoCA_Zmugd). The strain growth and the glucose consumption were monitored (Fig. 5).

The mutants with the selected overexpressions showed more variability between assays but the growth curve was similar to the control which indicates that the growth was not significantly affected by the additionally introduced modifications.

The chondroitin production in the end of fermentation (54 h) was evaluated for each engineered strain (Fig. 6).

The results obtained showed that *E. coli* K-12 MG1655 engineered with the chondroitin production pathway and *mltB* overexpression performed better in terms of extracellular chondroitin production, achieving a concentration of 427 ± 4 mg L^{-1} in 54 h. Regarding the yields per biomass or substrate consumption, both mutants expressing *mltB* or *sodA* showed better results compared to the control host. Although the differences between the control and *sodA* mutant are not significant (p-value > 0.05), *mltB*-overexpressing strain had improved yields of 1.7-fold, with statistically significant differences (p-value < 0.05) compared to the control host or to the *sodA* expressing mutant.

Chondroitin production in bioreactor (fed-batch experiments). The most promising mutant (*E. coli* K-12 MG1655 overexpressing *kfoC*, *kfoA*, *Zmugd* and *mltB*) was further cultivated under fed-batch conditions and compared to the control (strain without *mltB* overexpression). The growth and substrate consumption are described in Fig. 7.

As expected, the growth of engineered *E. coli* K-12 in the bioreactor was greatly improved by changing to fed-batch mode, compared to the fermentations in batch operation mode. However, this effect was more evident on the control strain (which showed a 2.1-fold increase in growth) than on the one overexpressing *mltB* (that exhibited only a 1.2-fold increase in growth).

The chondroitin production in the end of fermentation was also evaluated (Fig. 8).

Using the *E. coli* K-12 MG1655 engineered strains lacking or containing *mltB* overexpression, chondroitin concentration at the end of fed-batch fermentation achieved 621 ± 85 mg L^{-1} and 535 ± 52 mg L^{-1}, respectively. Despite the chondroitin production being lower in the mutant strain overexpressing the *mltB* gene, the yields on biomass and on glucose were higher (1.3-fold and 1.1-fold, respectively) compared to the parent mutant. This is justified with the lower growth of the *mltB*-expressing strain previously discussed (Fig. 7).

Chondroitin production has benefited from changing the operation mode to the fed-batch for both strains, resulting in 2.1 and 1.3-fold increase in chondroitin titers, for control and *mltB* strains, respectively. This is in accordance with other works in the literature that showed that fed-batch fermentations achieved the higher titers compared to batch or shake flask fermentations.[36,72,73,85] Although yields on biomass for both strains were lower than the ones obtained with batch, the yields on glucose were 2.2 and 1.4 times improved, for control and *mltB* strain, respectively. It is common for the fed-batch fermentations to result in much higher cell density, which occurred in this work, and if the growth is not accompanied by product formation at the same range, the yields in biomass are naturally lower. Nevertheless, when comparing both yields on biomass and on substrate, it is evident that the *mltB*-overexpressing strain was consistently the best performer.

Although *mltB* overexpression was not a logical modification to improve chondroitin production, it has been predicted in some solutions from computational optimization, including the one with the highest BPCY (solution 1, Table 2). In the batch experiments at the bioreactor scale, the *mltB*-overexpressing mutant was indeed the best performing strain in terms of chondroitin production and its growth capability was similar to the strain
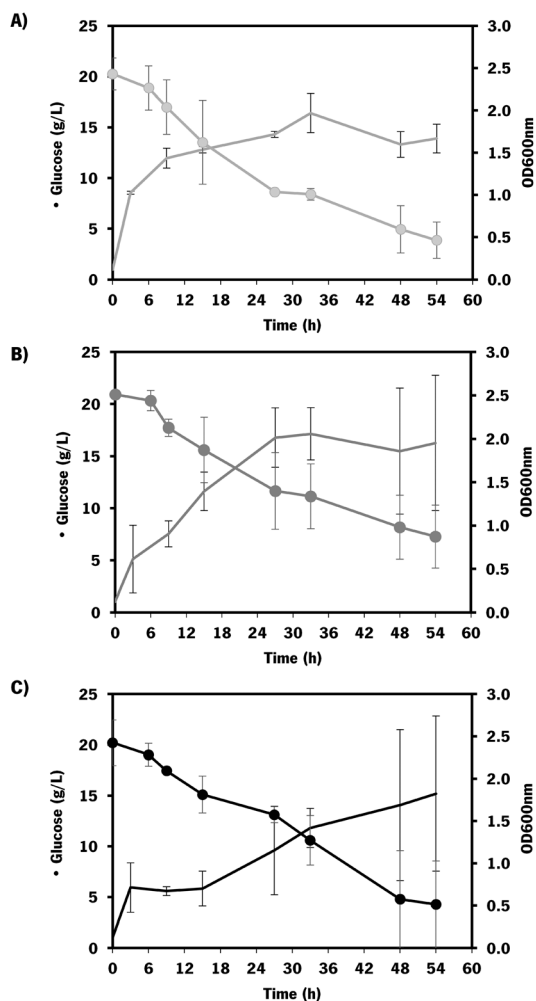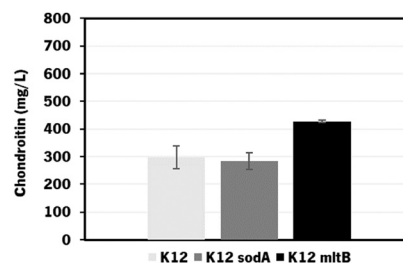
Fig. 8 Chondroitin production from cultured *E. coli* K-12 MG1655 harboring pRSFDuet_kfoCA_Zmugd (K12) and its counterpart with additional *mltB* overexpression, in bioreactors operated in fed-batch mode. The table shows a comparison of yield of chondroitin related to cell dry weight (CDW) and yield of chondroitin related to glucose, obtained for the different mutants.
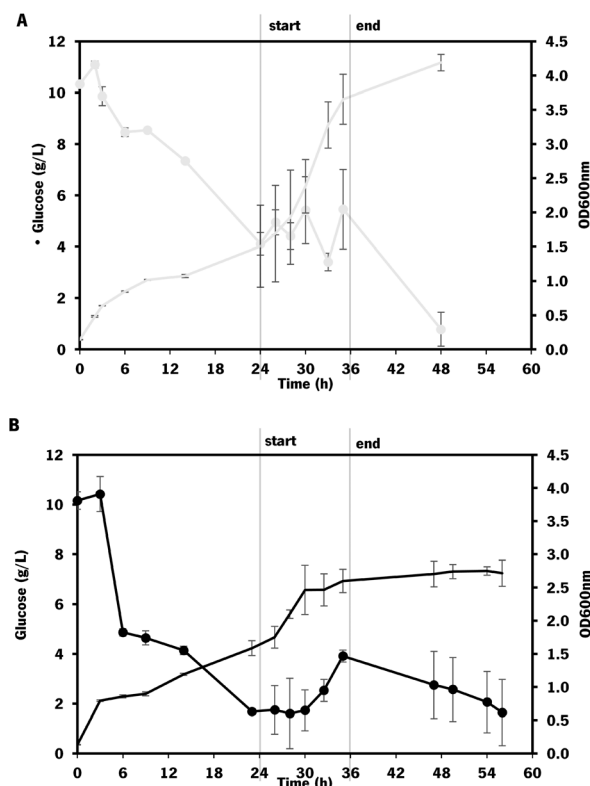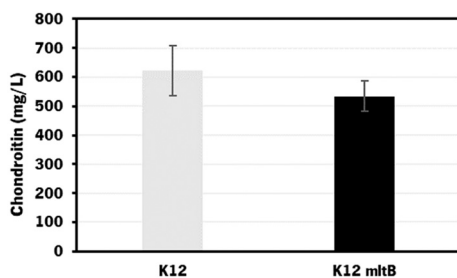
promoters such as the ones from the Anderson promoter collection, T7/*lac* constitutive systems (with *lacI* repressor deleted) or heat shock inducible promoters might be considered.[86–89]

The strain overexpressing *mltB* presented the best chondroitin yields in bioreactors when operated in both batch and fed-batch modes, which suggests that a slight improvement in the peptidoglycan recycling can redirect the metabolic flux towards the chondroitin precursor production.

Conclusions

In the current study, genome-scale metabolic models' optimizations were used for the first time to identify genes for under- and overexpression, which allowed the selection of possible targets to improve chondroitin production. The suggested promising mutants were further validated *in vivo* by constructing the *E. coli* mutant strains containing the chondroitin heterologous pathway and the additionally selected modifications. In flask fermentation, *E. coli* harboring the biosynthetic pathway was able to produce 62 mg L^{-1} of chondroitin. The evaluated mutants with additional modifications on this engineered strain resulted in chondroitin titers from 42 to 118 mg L^{-1}. In the bioreactor, batch fermentations led to an enhanced chondroitin production, with the highest titer achieved by *E. coli* K-12 overexpressing *mltB* (427 mg L^{-1} in 54 h). Further fed-batch assays resulted in an improvement up to 535 mg L^{-1} of chondroitin production. This study highlights new possible metabolic engineering targets to improve chondroitin production which ultimately can contribute to advancing the biotechnological production of this most sought glycosaminoglycan.

Author contributions

Márcia R. Couto: investigation; formal analysis; validation; visualization; writing – original draft; writing – review & editing. Joana L. Rodrigues: conceptualization; supervision; study coordination; writing – review & editing. Adelaide Braga: supported bioreactor experiments; writing – review & editing. Oscar Dias: supported *in silico* experiments; writing – review & editing. Lígia Rodrigues: conceptualization; funding acquisition; supervision; project administration; writing – review & editing.

Conflicts of interest

There are no conflicts to declare.

Acknowledgements

References

1 E. J. O'Brien, J. M. Monk and B. O. Palsson, *Cell*, 2015, **161**, 971–987.
2 C. Gu, G. B. Kim, W. J. Kim, H. U. Kim and S. Y. Lee, *Genome Biol.*, 2019, **20**, 1–18.
3 A. Oliveira, J. Rodrigues, E. C. Ferreira, L. Rodrigues and O. Dias, *PLoS Comput. Biol.*, 2021, **17**, e1008704.
4 C. J. Norsigian, N. Pusarla, J. L. McConn, J. T. Yurkovich, A. Dräger, B. O. Palsson and Z. King, *Nucleic Acids Res.*, 2020, **48**, D402–D406.
5 D. Segrè, D. Vitkup and G. M. Church, *Proc. Natl. Acad. Sci. U. S. A.*, 2002, **99**, 15112–15117.
6 S. A. Becker, A. M. Feist, M. L. Mo, G. Hannum, B. Palsson and M. J. Herrgard, *Nat. Protoc.*, 2007, **2**, 727–738.
7 J. Schellenberger, R. Que, R. M. T. Fleming, I. Thiele, J. D. Orth, A. M. Feist, D. C. Zielinski, A. Bordbar, N. E. Lewis, S. Rahmanian, J. Kang, D. R. Hyduke and B. Palsson, *Nat. Protoc.*, 2011, **6**, 1290–1307.
8 P. Maia, M. Rocha and I. Rocha, *Microbiol. Mol. Biol. Rev.*, 2016, **80**, 45–67.
9 A. P. Burgard, P. Pharkya and C. D. Maranas, *Biotechnol. Bioeng.*, 2003, **84**, 647–657.
10 P. Pharkya, A. P. Burgard and C. D. Maranas, *Genome Res.*, 2004, **14**, 2367–2376.
11 K. R. Patil, I. Rocha, J. Förster, J. Nielsen, J. Forster and J. Nielsen, *BMC Bioinf.*, 2005, **6**, 1–12.
12 M. Rocha, P. Maia, R. Mendes, J. P. Pinto, E. C. Ferreira, J. Nielsen, K. R. Patil and I. Rocha, *BMC Bioinf.*, 2008, **9**, 1–16.
13 G. Melzer, M. E. Esfandabadi, E. Franco-Lara and C. Wittmann, *BMC Syst. Biol.*, 2009, **3**, 1–16.

14 J. Kim and J. L. Reed, *BMC Syst. Biol.*, 2010, **4**, 53.

15 S. Ranganathan, P. F. Suthers and C. D. Maranas, *PLoS Comput. Biol.*, 2010, **6**, e1000744.

16 S. Ranganathan, T. W. Tee, A. Chowdhury, A. R. Zomorrodi, J. M. Yoon, Y. Fu, J. V. Shanks and C. D. Maranas, *Metab. Eng.*, 2012, **14**, 687–704.

17 J. M. Otero, D. Cimini, K. R. Patil, S. G. Poulsen, L. Olsson and J. Nielsen, *PLoS One*, 2013, **8**, 1–10.

18 N. Guan, B. Du, J. Li, H. D. Shin, R. R. Chen, G. Du, J. Chen and L. Liu, *Biotechnol. Bioeng.*, 2018, **115**, 483–494.

19 G. Xu, W. Zou, X. Chen, N. Xu, L. Liu and J. Chen, *PLoS One*, 2012, **7**, 1–10.

20 X. Chen, G. Xu, N. Xu, W. Zou, P. Zhu, L. Liu and J. Chen, *Metab. Eng.*, 2013, **19**, 10–16.

21 M. Kim, B. G. Park, E. J. Kim, J. Kim and B. G. Kim, *Biotechnol. Biofuels*, 2019, **12**, 1–14.

22 P. Mishra, N.-R. Lee, M. Lakshmanan, M. Kim, B.-G. Kim and D.-Y. Lee, *BMC Syst. Biol.*, 2018, **12**, 12.

23 M. Kavšček, G. Bhutada, T. Madl and K. Natter, *BMC Syst. Biol.*, 2015, **9**, 1–13.

24 J. E. Yang, S. J. Park, W. J. Kim, H. J. Kim, B. J. Kim, H. Lee, J. Shin and S. Y. Lee, *Nat. Commun.*, 2018, **9**, 79.

25 K. R. Kildegaard, N. B. Jensen, K. Schneider, E. Czarnotta, E. Özdemir, T. Klein, J. Maury, B. E. Ebert, H. B. Christensen, Y. Chen, I. K. Kim, M. J. Herrgård, L. M. Blank, J. Forster, J. Nielsen and I. Borodina, *Microb. Cell Fact.*, 2016, **15**, 1–13.

26 I. Borodina, K. R. Kildegaard, N. B. Jensen, T. H. Blicher, J. Maury, S. Sherstyk, K. Schneider, P. Lamosa, M. J. Herrgård, I. Rosenstand, F. Öberg, J. Forster and J. Nielsen, *Metab. Eng.*, 2015, **27**, 57–64.

27 J. Zhang, S. D. Petersen, T. Radivojevic, A. Ramirez, A. Pérez-Manríquez, E. Abeliuk, B. J. Sánchez, Z. Costello, Y. Chen, M. J. Fero, H. G. Martin, J. Nielsen, J. D. Keasling and M. K. Jensen, *Nat. Commun.*, 2020, **11**, 4880.

28 S. Ferreira, R. Pereira, S. A. Wahl and I. Rocha, *Biotechnol. Bioeng.*, 2020, **117**, 2571–2587.

29 P. Xu, S. Ranganathan, Z. L. Fowler, C. D. Maranas and M. A. G. G. Koffas, *Metab. Eng.*, 2011, **13**, 578–587.

30 F. Cheng, H. Yu and G. Stephanopoulos, *Metab. Eng.*, 2019, **55**, 276–289.

31 M. R. Couto, J. L. Rodrigues and L. R. Rodrigues, *Biotechnol. Rep.*, 2022, **33**, e00710.

32 V. Vassallo, A. Stellavato, D. Cimini, A. V. A. Pirozzi, A. Alfano, M. Cammarota, G. Balato, A. D'Addona, C. Ruosi and C. Schiraldi, *J. Cell. Biochem.*, 2020, **122**, 1021–1036.

33 A. Stellavato, V. Tirino, F. Novellis, A. Della Vecchia, F. Cinquegrani, M. Rosa, G. Papaccio and C. Schiraldi, *J. Cell. Biochem.*, 2016, **2169**, 2158–2169.

34 N. Alessio, A. Stellavato, D. Aprile, D. Cimini, V. Vassallo, G. Di Bernardo, U. Galderisi and C. Schiraldi, *Front. Cell Dev. Biol.*, 2021, **9**, 1–10.

35 D. Cimini, S. Boccella, A. Alfano, A. Stellavato, S. Paino, C. Schiraldi, F. Guida, M. Perrone, M. Donniacuo, V. Tirino, V. Desiderio and B. Rinaldi, *Front. Bioeng. Biotechnol.*, 2022, **10**, 1–12.

36 W. He, L. Fu, G. Li, J. A. Jones, R. J. Linhardt, M. Koffas, J. A. Jones, R. J. Linhardt, M. Koffas, J. A. Jones, R. J. Linhardt and M. Koffas, *Metab. Eng.*, 2015, **27**, 92–100.

37 I. Rocha, P. Maia, P. Evangelista, P. Vilaça, S. Soares, J. P. Pinto, J. Nielsen, K. R. Patil, E. C. Ferreira and M. Rocha, *BMC Syst. Biol.*, 2010, **4**, 1–12.

38 N. E. Lewis, K. K. Hixson, T. M. Conrad, J. A. Lerman, P. Charusanti, A. D. Polpitiya, J. N. Adkins, G. Schramm, S. O. Purvine, D. Lopez-Ferrer, K. K. Weitz, R. Eils, R. König, R. D. Smith and B. Ø. Palsson, *Mol. Syst. Biol.*, 2010, **6**, 1–13.

39 V. Pereira, F. Cruz and M. Rocha, *Bioinformatics*, 2021, 1–3.

40 K. Deb, A. Pratap, S. Agarwal and T. Meyarivan, *IEEE Trans. Evol. Comput.*, 2002, **6**, 182–197.

41 R. Mahadevan and C. H. Schilling, *Metab. Eng.*, 2003, **5**, 264–276.

42 O. F. Restaino, I. di Lauro, R. Di Nuzzo, M. De Rosa, C. Schiraldi, R. Di Nuzzo, M. De Rosa, C. Schiraldi, R. Di Nuzzo, M. De Rosa and C. Schiraldi, *Biosci. Rep.*, 2017, **37**, 1–12.

43 P. Jin, L. Zhang, P. Yuan, Z. Kang, G. Du and J. Chen, *Carbohydr. Polym.*, 2016, **140**, 424–432.

44 D. Cimini, M. De Rosa, A. Viggiani, O. F. Restaino, E. Carlino and C. Schiraldi, *J. Biotechnol.*, 2010, **150**, 324–331.

45 H. Yu and G. Stephanopoulos, *Metab. Eng.*, 2008, **10**, 24–32.

46 M. R. Couto, J. L. Rodrigues and L. R. Rodrigues, *Life*, 2021, **11**, 1201.

47 B. F. Cress, O. D. Toparlak, S. Guleria, M. Lebovich, J. T. Stieglitz, J. A. Englaender, J. A. Jones, R. J. Linhardt and M. A. G. G. Koffas, *ACS Synth. Biol.*, 2015, **4**, 987–1000.

48 C. R. Reisch and K. L. J. Prather, *Sci. Rep.*, 2015, **5**, 15096.

49 D. R. Nielsen, S. H. Yoon, C. J. Yuan and K. L. J. Prather, *Biotechnol. J.*, 2010, **5**, 274–284.

50 T. Bitter and H. M. Muir, *Anal. Biochem.*, 1962, **4**, 330–334.

51 G. L. Miller, *Anal. Chem.*, 1959, **31**(3), 426–428.

52 J. Wu, Q. Zhang, L. Liu, X. Chen, J. Liu and Luo, Recombinant Escherichia coli for high efficiency production of fructosylated chondroitin and method for making thereof, *US Pat.*, 10508279B2, 2019.

53 J. E. Woo, H. J. Seong, S. Y. Lee and Y. S. Jang, *Front. Bioeng. Biotechnol.*, 2019, **7**, 1–9.

54 Q. Cheng and J. T. Park, *J. Bacteriol.*, 2002, **184**, 6434–6436.

55 M. Lee, D. Hesek, L. I. Llarrull, E. Lastochkin, H. Pi, B. Boggess and S. Mobashery, *J. Am. Chem. Soc.*, 2013, **135**, 3311–3314.

56 D. A. Dik, D. R. Marous, J. F. Fisher and S. Mobashery, *Crit. Rev. Biochem. Mol. Biol.*, 2017, **52**, 503–542.

57 J. T. Park and T. Uehara, *Microbiol. Mol. Biol. Rev.*, 2008, **72**, 211–227.

58 A. Maqbool, V. M. Levdikov, E. V. Blagova, M. Hervé, R. S. P. Horler, A. J. Wilkinson and G. H. Thomas, *J. Biol. Chem.*, 2011, **286**, 31512–31521.

59 J. Fricke, J. Neuhard, R. A. Kelln and S. Pedersen, *J. Bacteriol.*, 1995, **177**, 517–523.

60 J. Landberg, N. R. Wright, T. Wulff, M. J. Herrgård and A. T. Nielsen, *Biotechnol. Bioeng.*, 2020, **117**, 3835–3848.

610 | *Mol. Syst. Des. Eng.*, 2024, **9**, 597–611

This journal is © The Royal Society of Chemistry and IChemE 2024

61 N. Bucurenci, H. Sakamoto, P. Briozzo, N. Palibroda, L. Serina, R. S. Sarfati, G. Labesse, G. Briand, A. Danchin, O. Bârzu and A. M. Gilles, *J. Biol. Chem.*, 1996, **271**, 2856–2862.

62 P. Meyer, C. Evrin, P. Briozzo, N. Joly, O. Bârzu and A. M. Gilles, *J. Biol. Chem.*, 2008, **283**, 36011–36018.

63 H. Sakamoto, S. Landais, C. Evrin, C. Laurent-Winter, O. Bârzu and R. A. Kelln, *Microbiology*, 2004, **150**, 2153–2159.

64 J. T. Park, J. H. Shim, P. L. Tran, I. H. Hong, H. U. Yong, E. F. Oktavina, H. D. Nguyen, J. W. Kim, T. S. Lee, S. H. Park, W. Boos and K. H. Park, *J. Bacteriol.*, 2011, **193**, 2517–2526.

65 G. Vadlamani, K. A. Stubbs, J. Désiré, Y. Blériot, D. J. Vocadlo and B. L. Mark, *Protein Sci.*, 2017, **26**, 1161–1170.

66 A. Roberts, S. Y. Lee, E. McCullagh, R. E. Silversmith and D. E. Wemmer, *Proteins: Struct., Funct., Genet.*, 2005, **58**, 790–801.

67 M. Zhao, Y. Li, F. Wang, Y. Ren and D. Wei, *Synth. Syst. Biotechnol.*, 2022, **7**, 982–988.

68 A. M. Olajuyin, M. Yang, Y. Liu, T. Mu, J. Tian, O. A. Adaramoye and J. Xing, *Bioresour. Technol.*, 2016, **214**, 653–659.

69 C. D. Lu, Y. Y. Xiong, J. F. Zhao and J. H. Wang, *Adv. Mater. Res.*, 2015, **1088**, 503–506.

70 A. Negrete and J. Shiloach, *Microb. Cell Fact.*, 2017, **16**, 1–12.

71 A. Badri, A. Williams, A. Awofiranye, P. Datta, K. Xia, W. He, K. Fraser, J. S. Dordick, R. J. Linhardt and M. A. G. G. Koffas, *Nat. Commun.*, 2021, **12**, 1–10.

72 M. De Rosa, C. Schiraldi and D. Cimini, Biotechnological production of chondroitin, *US Pat.*, 8592186B2, 2013.

73 D. Cimini, M. De Rosa, E. Carlino, A. Ruggiero and C. Schiraldi, *Microb. Cell Fact.*, 2013, **12**, 1.

74 D. Cimini, R. Russo, S. D'Ambrosio, I. Dello Iacono, C. Rega, E. Carlino, O. Argenzio, L. Russo, B. D'Abrosca, A. Chambery and C. Schiraldi, *Biotechnol. Bioeng.*, 2018, **115**, 1801–1814.

75 Q. Wu, A. Yang, W. Zou, Z. Duan, J. Liu, J. Chen and L. Liu, *Biotechnol. Prog.*, 2013, **29**, 1140–1149.

76 K. Suzuki, K. Miyamoto and H. Kaseyama, Chondroitin-producing bacterium and method of producing chondroitin, *US Pat.*, 8283145B2, 2012.

77 D. Cimini, I. Dello Iacono, E. Carlino, R. Finamore, O. F. Restaino, P. Diana, E. Bedini and C. Schiraldi, *AMB Express*, 2017, **7**, 1–11.

78 F. Cheng, S. Luozhong, H. Yu and Z. Guo, *J. Microbiol. Biotechnol.*, 2019, **29**, 392–400.

79 X. Jin, W. Zhang, Y. Wang, J. Sheng, R. Xu, J. Li, G. Du and Z. Kang, *Green Chem.*, 2021, **23**, 4365–4374.

80 M. E. Chung, I. H. Yeh, L. Y. Sung, M. Y. Wu, Y. P. Chao, I. S. Ng and Y. C. Hu, *Biotechnol. Bioeng.*, 2017, **114**, 172–183.

81 Q. Cheng, H. Li, K. Merdek and J. T. Park, *J. Bacteriol.*, 2000, **182**, 4836–4840.

82 D. Yu, H. M. Ellis, E. C. Lee, N. A. Jenkins, N. G. Copeland and D. L. Court, *Proc. Natl. Acad. Sci. U. S. A.*, 2000, **97**, 5978–5983.

83 S. Dhar, H. Kumari, D. Balasubramanian and K. Mathee, *J. Med. Microbiol.*, 2018, **67**, 1–21.

84 W. Vötsch and M. F. Templin, *J. Biol. Chem.*, 2000, **275**, 39032–39038.

85 D. Cimini, S. Fantaccione, F. Volpe, M. De Rosa, O. F. Restaino, G. Aquino and C. Schiraldi, *Appl. Microbiol. Biotechnol.*, 2014, **98**, 3955–3964.

86 J. L. Rodrigues and L. R. Rodrigues, *Trends Biotechnol.*, 2018, **36**, 186–198.

87 J. L. Rodrigues, M. Sousa, K. L. J. Prather, L. D. Kluskens and L. R. Rodrigues, *J. Biotechnol.*, 2014, **188**, 67–71.

88 V. Menart, S. Jevševar, M. Vilar, A. Trobiš and A. Pavko, *Biotechnol. Bioeng.*, 2003, **83**, 181–190.

89 D. Koma, T. Kishida, H. Yamanaka, K. Moriyoshi, E. Nagamori and T. Ohmoto, *J. Biosci. Bioeng.*, 2018, **126**, 586–595.

This journal is © The Royal Society of Chemistry and IChemE 2024

Mol. Syst. Des. Eng., 2024, **9**, 597–611 | **611**